Coadsorption of Human Milk Lactoferrin into the Dipalmitoylglycerolphosphatidylcholine Phospholipid Monolayer Spread at the Air/Water Interface

Fausto Miano,* Xiubo Zhao,† Jian R. Lu,† and Jeff Penfold‡

*Società Industria Farmaceutica Italiana SpA, Lavinaio (Catania), Italy; †Biological Physics Group, School of Physics and Astronomy, The University of Manchester, Sackville Street Building, Manchester M60 1QD, United Kingdom; and ‡ISIS Facility, Rutherford Appleton Laboratory, The Council for the Central Laboratory of the Research Councils, Chilton, Didcot OX11 0QZ, United Kingdom

ABSTRACT The coadsorption of human milk lactoferrin into a spread monolayer of dipalmitoylglycerol phosphatidylcholine (DPPC) at the air/water interface has been studied by neutron reflection. The system is a good model of the preocular tear film outer interface, which was the motivation for the study. The association of the protein with the surface was indicated by an increase of the surface pressure exerted by the DPPC monolayer. The extent of lactoferrin coadsorption was found to decrease with increasing surface pressure in the lipid monolayer, a trend consistent with the observation reported for other proteins, such as lysozyme and β-lactoglobulin. The neutron reflectivity measurements were subsequently carried out at the three surface pressures of 8, 15, and 35 mN/m to examine the structure and composition of lactoferrin coadsorbed at the interface. Whereas the DPPC monolayer effectively prevented lactoferrin insertion at the high surface pressure, a measurable amount of lactoferrin was found at the air/water interface at the two lower surface pressures. At 15 mN/m it was difficult to identify the distribution of lactoferrin with respect to the DPPC monolayer, due to its relatively low adsorbed amount and much broader distribution. At the lowest surface pressure of 8 mN/m, the lactoferrin coadsorption was found to increase with time over the first few hours. After 5 h the distribution of the lactoferrin layer became similar to, though quantitatively lower than, that adsorbed in the absence of the DPPC monolayer. It is characterized by a top dense sublayer of 15 Å with a bottom diffuse sublayer of 60 Å, indicating structural unfolding induced by surface adsorption under these conditions.

INTRODUCTION

The anterior part of the eye is characterized by the presence of a wetting tear film that is spread by the mechanical action of eyelid blinking. The tear film exerts a protective and washing action upon the corneal and conjunctival epithelia, contributing to the maintenance of ocular comfort. Any disorder in the tear film leads to damage to the ocular surface and is associated with symptoms of ocular discomfort and, in the long run, to ''dry eye'' syndrome. The delicate nature of this biological interface has inspired many research workers in the field, who have proposed the concept of a three-layer tear film where mucin is an integral part attached to the glycocalyx of the ocular epithelia in an aqueous fluid containing electrolytes, small organic compounds, and proteins (1,2). Lysozyme, lactoferrin, secretory IgA, and tear lipocalin are involved in corneal and conjunctival epithelium defense. This specific tear composition is well adapted to the protective function of the ocular epithelia (3,4).

At the outer fluid/air interface, a lipid layer secreted by the meibomian glands located in the lid margins is associated with several biological functions, and its physical effects include the lubrication of tear film, the alleviation of the movement of the eyelids during a blink, the supply of a barrier to the entry of microorganisms and organic matter such as pollen, the stabilization of the film against thinning, and the depletion of evaporation from the aqueous phase (5,6). The latter effect has for a long time been emphasized and a considerable number of patients have been diagnosed for evaporative dry eye. Recent studies indicated that an insufficient amount of tear lipid layer leads to the abnormal evaporative tear loss and unstable tear film on the ocular surface of patients with obstructive meibomian gland dysfunction (7). However, the increased rate of evaporation is still lower than that produced by changes of environmental conditions such as temperature and relative humidity, which affect the tear evaporation rate in a more remarkable manner as reported in an in vitro model (8). In addition, it has been suggested that defects in the lipid layer itself could be responsible for tear breakup and subsequent dry spots (9). Although recent research has produced a much better understanding of meibum functionality, to our knowledge a general description of how component lipids are important in terms of the whole tear film functionality is not yet achieved (10). In particular, studies concerning the interactions between tear proteins and lipids do not seem to provide a comprehensive picture of how tear proteins mechanistically interact with the lipid film (11) or function as lipid scavengers (12).

In analogy with the more advanced studies in the field of pulmonary surfactants (13–15), the biophysical properties of the tear film composed of phosphatidylcholine, cholesterol, sphingomyelin, and proteins can be modeled in monolayer experiments (16,17). These amphiphiles form reversibly

Submitted March 8, 2006, and accepted for publication October 10, 2006.

Address reprint requests to Jian R. Lu, Tel.: 44-161-2003926; E-mail: j.lu@Manchester.ac.uk.

0006-3495/07/02/1254/09 $2.00

doi: 10.1529/biophysj.105.078592

compressible and expandable monomolecular films at the air/water interface, a prerequisite for the imitation of the tear film produced normally by meibomian glands (18,19). Moreover, studies concerning association or penetration of proteins at the air/aqueous interface may be formed on a firm theoretical and experimental ground (20–22). The coadsorption of proteins to the interface has been widely reported to contribute to the further increase in surface pressure, depending upon the initial surface pressure produced by the lipids, but the molecular mechanistic processes underlying the actions of the proteins remain elusive.

The purpose of this experimental work is to investigate the interactions between a model lipid monolayer and lactoferrin, a typical tear protein. Dipalmitoylglycerolphosphatidylcholine (DPPC) was chosen because its monolayer properties can be carefully tuned in a way that makes it possible to define the molecular density by varying the area per molecule on a Langmuir trough. Lactoferrin, which is a bilobal iron-binding glycoprotein also distributed in other physiological fluids like milk, saliva, and semen and in neutrophils and granulocytes cells, bears several physiological functions derived from its iron-binding properties. Lactoferrin is known to exhibit an antimicrobial property and mediate some effects of inflammation (23). In patients with dry eye, lactoferrin is usually altered in comparison to its level in healthy subjects (24,25). Lactoferrin is able to adsorb at the air/aqueous interface with concomitant loss of tertiary structure (26), whereas other tear proteins like lysozyme retain their conformations (27).

Neutron reflectivity coupled with the Langmuir trough study appears to be a highly suitable technique to investigate the coadsorption of lactoferrin onto the DPPC monolayer to verify if lactoferrin will retain its conformation at the interface in the presence of a lipid film spread upon the aqueous phase. Results will be discussed in terms of tear lipids versus protein's interactions.

EXPERIMENTAL METHODS

The neutron reflectivity measurements were carried out at Rutherford Appleton Laboratory near Oxford, UK, using reflectometer SURF. The instrument used a white neutron beam with wavelengths ranging from 0.5 to 6.5 Å. Each reflectivity profile was measured at three different beam incidence angles of 0.5°, 0.8°, and 1.5°, and the combined reflectivity profile covered a wave vector range (κ) from 0.015 to 0.5 $Å^{-1}$. The instrument was calibrated from fitting to the pure D_2O profile measured at an incidence angle of 1.5°. Constant background arising from incoherent scattering was subtracted using the measured reflectivity averaged over 0.3–0.5 $Å^{-1}$. The typical background in null reflecting water (NRW) was 5×10^{-6} and that in D_2O 2×10^{-6}. A Nima (Nima Technology Ltd, Coventry, UK) trough was used in the neutron reflectivity study. The carrier solvent used to facilitate the spreading of the lipid sample onto the surface of the Nima trough contained 90% $CHCl_3$ and 10% CH_3CH_2OH. The neutron reflectivity profiles were measured at three fixed surface pressures of 8, 15, and 35 mN/m, with and without injection of lactoferrin. Human milk lactoferrin (Sigma, Milan, Italy) was dissolved in water and injected into the subphase of the spread DPPC monolayer in the form of 1 mg/ml solution in either NRW or D_2O. The concentration of NaCl in the aqueous phase was fixed at 0.3 M throughout the experiments to match the physiological conditions. Both d- and h-DPPC were synthesized by Larodan (Malmö, Sweden). Deuteration was made to the two acyl chains only containing 62 D in each d-DPPC molecule. The scattering lengths (b_L), volume, and scattering length densities (ρ) for the constituting fragments of the lipids and lactoferrin are given in Table 1.

D_2O (99.9% D content) used was purchased from Sigma and was used as supplied. Ultrapure water (Ulgastat ultrapure) was used throughout the experiment for solution preparation and also for final glassware rinsing before drying. The sodium chloride used was AR grade purchased from Aldrich (Dorset, Uk) and used as supplied. Unless stated all the experiments were carried out at 20–22°C.

RESULTS AND DISCUSSION

Surface pressure measurements

Before the neutron reflectivity measurements, the surface pressure (π)-area (A) isotherms were measured for both deuterated dipamitoylglycerolphosphotidylcholine (d-DPPC) and hydrogenated sample (h-DPPC), with the results shown in Fig. 1. The isotherm was obtained from steadily reducing the area between Langmuir trough barriers at a rate corresponding to 2 cm^2/min.

Fig. 1 shows two distinct regions of the dependence of π on A, the flat region where π shows a slow variation with respect to A and the almost vertical region where π follows a fast response with respect to A. Some isotopic effect is clearly visible between the two versions of labeled compounds, particularly below 15 mN/m, consistent with the observation reported in the open literature (28). Fig. 1 also shows a clear hysteresis from the d-DPPC curve between compression and expansion, indicating the effect of molecular relaxation on A. It was found that reduction in the rates of compression and expansion could reduce this discrepancy, but typical inconsistency in A between parallel compressions for a given DPPC was found to be $\sim\pm 6$ $Å^2$. Neutron reflection independently determined A with a much better resolution, as will be discussed later, but the time-dependent molecular relaxation meant that the area per molecule obtained from neutron reflectivity was a timed averaged value.

Coadsorption of protein into a spread lipid monolayer tends to increase surface pressure. The extent of π increase at constant area was examined using a Nima trough with the lactoferrin concentration fixed at 0.1 mg/ml (equivalent to 10^{-5} M) corresponding to the critical micellar concentration. Fig. 2 shows the surface pressure arising from the addition of lactoferrin plotted versus time starting from the initial surface pressure exerted by a previously spread DPPC monolayer. It can be seen from Fig. 2 that as the DPPC monolayer surface pressure increases, the pressure difference arising from protein adsorption decreases. At the initial surface pressure of 35 mN/m, no change in surface pressure relating to protein adsorption was observed, indicating that at or above this pressure the protein does not coadsorb into the interface any longer.

Fig. 2 also shows the gradual rising of surface pressure with time in the presence of lactoferrin. The time-dependent

TABLE 1 Physical constants for lactoferrin and fragments constituting d-DPPC and h-DPPC

Segment	b_L/Å	Volume/Å^3	ρ/Å^{-2}
$C_{15}H_{31}COO-$	2.1×10^{-5}	465	0.05×10^{-6}
$C_{15}D_{31}COO-$	3.22×10^{-3}	465	6.91×10^{-6}
$-CH_2CHCH_2-$	1.25×10^{-5}	80	0.15×10^{-6}
$-PO_4^-C_2H_4N^+(CH_3)_3$	22.3×10^{-5}	290	0.77×10^{-6}
Lactoferrin in NRW	0.190	93600	2.03×10^{-6}
Lactoferrin in D_2O	0.315	93600	3.36×10^{-6}

effect is related to the initial surface pressure applied and to the concentration of lactoferrin in the aqueous subphase as already reported in a previous study (11). At the high initial surface pressure of 35 mN/m, there is little drifting of the surface pressure because there is little protein adsorption. As the initial surface pressure becomes lower, more protein starts to coadsorb and it takes longer for the adsorption to reach equilibration. At the lowest initial surface pressure of 8 mN/m, it takes 6 h for the surface pressure to plateau, comparable to the timescale for surface equilibration observed for β-lactoglobulin as reported by Zhao et al. (29).

The penetration of soluble components into an insoluble lipid monolayer has been extensively studied and reported (21). Many studies have focused on investigating the kinetic and equilibrium properties of different penetration systems, with a number of more recent studies reporting interesting two-dimensional (2D) morphological structures using complementary techniques such as Brewster angle microscopy (BAM). BAM is sensitive to the in-plane orientational disorder owing to the optical anisotropy induced by the tilted aliphatic chains. A number of studies have reported that the first-order phase transition in a fluid expanded the DPPC monolayer as a result of penetration of β-lactoglobulin (29). Association of soluble proteins into phospholipid monolayers could cause fluorescence quenching of membrane-bound fluorophores by fluorescence microscopy. X-ray reflectivity and glancing incidence x-ray diffraction (GIXD) have also been carried out to obtain information on the structure of penetrated monolayers (21).

In this work the objective is to exploit the ability of neutron reflectivity in revealing complementary structural information for this type of mixed monolayer and, more specifically, to determine the structure and amount of the coadsorbed protein.

Neutron reflection

Neutron reflectivity was first measured on a monolayer of acyl chain deuterated d-DPPC spread upon an NRW subphase. Under this isotopic contrast, the reflectivity arises from the lipid monolayer only and the water substrate makes no contribution to the specular signal. Because the scattering length densities from the hydrogenated glycerol backbone and the phosphocholine (PC) head are very low, their contributions under this contrast are negligible. Thus the measurements under this isotopic contrast offer a direct estimate of the thickness of the dipalmitoyl chain region.

Fig. 3 shows the reflectivity profiles measured at the three surface pressures of 8, 15, and 35 mN/m. These surface pressures correspond to an area per molecule of 80 $\pm$ 10, 50 $\pm$ 6, and 40 $\pm$ 4 Å^2, according to the results shown in Fig. 1 for d-DPPC. These values were obtained from the Langmuir trough measurements and allowed a direct comparison with the neutron data. Surface pressure increase leads to the rise in surface packing density, corresponding to the reduction in area per molecule and also to the increase in layer thickness. The former is shown in the increased level of the reflectivity profile, whereas the latter is reflected in the increased slope of the curve.

Quantitative information about area per molecule (A) and layer thickness can be obtained from either model fitting

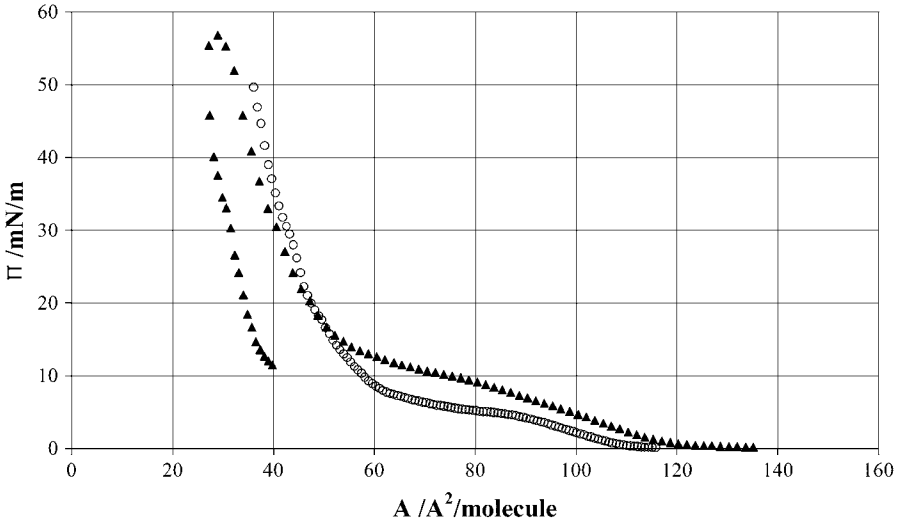

FIGURE 1 Surface pressure (π) versus area per molecule (A) obtained from the Langmuir trough experiment at 25°C (*open circles*) is h-DPPC and (*solid triangles*) is d-DPPC.

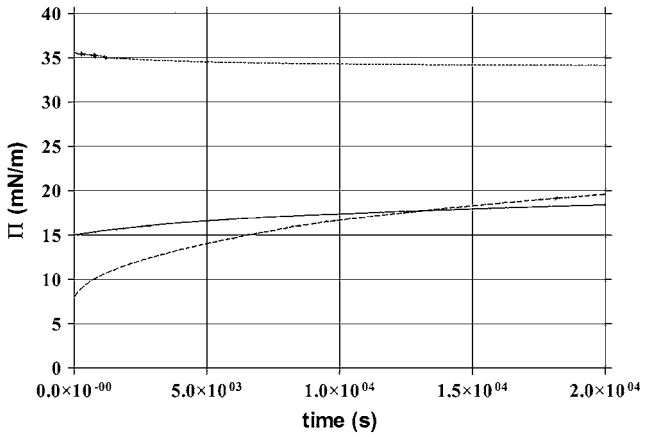

FIGURE 2 Surface pressure change with time due to coadsorption of lactoferrin from aqueous solution ($C = 1.0$ g/L) plotted at three initial surface pressures of the DPPC monolayer (8 mN/m (*low*), 15 mN/m (*middle*), and 35 mN/m (*upper*)).

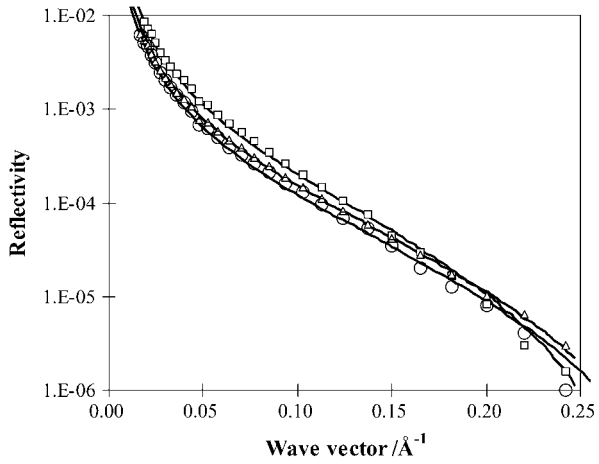

FIGURE 3 Neutron reflectivity profiles measured from surface adsorption of d-DPPC on the NRW surface at the surface pressure of 8 (*open circles*), 15 (*open triangles*), and 35 (*open squares*) mN/m. The continuous lines represent the best uniform layer fits with structural parameters listed in Table 2.

based on the optical matrix formula or direct calculation based on the kinematic approach (30). As found previously, although BAM has revealed 2D heterogeneity within the DPPC monolayers over the pressure range studied, all the reflectivity profiles measured under NRW could be fitted by a uniform layer model (28). In the kinematic approach, reflectivity (R) is related to the thickness and composition through the following equation

$$h_{\mathrm{pp}}(\kappa)\kappa^2 = \frac{R\kappa^4}{16\pi^2 b_{\mathrm{L}}^2} = \frac{4}{A^2\tau^2}\sin^2\left(\frac{\kappa\tau}{2}\right), \qquad (1)$$

where $h_{\mathrm{pp}}(\kappa)$ is the self partial structure factor for DPPC, $\kappa = 4\pi\sin\theta/\lambda$ (θ is the beam incidence angle, and λ is the wavelength), b_{L} is the scattering length of DPPC, τ is the layer thickness, and A is the area per molecule. Eq. 1 contains both τ and A as variables, but change in A affects the level of the reflectivity and change in τ affects its shape. Thus Eq. 1 can be used to derive reliable information about A and τ from any measured reflectivity. The continuous lines shown in Fig. 3 were calculated by adjusting τ and A to produce a good fit for each measured reflectivity profile. The resultant τ and A pairs from neutron reflectivity together with the average A values obtained from Langmuir trough measurements are shown in Table 2.

Model fitting based on an optical matrix formula is a more widely applied method. The best uniform layer fit is usually obtained by comparing the calculated profile with the measured one, and the fitting process was iterated until an acceptable fit was obtained. The uniform layer model fit produces τ and scattering length density (ρ) from which A can be obtained via

$$A = \frac{b_L}{\rho\tau}, \qquad (2)$$

where b_{L} is the scattering length for the phospholipids. It was found that within experimental error the two approaches produced the optimal fits with almost identical structural parameters. The quality of the fits from the uniform layer model is clearly seen from the consistency between the measured data and the calculated reflectivity profiles. The difference in A as obtained from the two parallel neutron data analyses at each surface pressure was well within ± 4 Å^2. The A values obtained from neutron reflection were thus 70, 55, and 45 Å^2, with the order of increasing surface pressure, and these compare well with 80 ± 10, 50 ± 6, and 40 ± 4 Å^2 from the Langmuir trough experiments. The differences are within the acceptable experimental error given that the errors from the Langmuir trough work could be greater.

Although the uniform layer model fitted the measured reflectivity profiles well, the Gaussian model is more realistic and more appropriate for approximating the structural distribution of surface monolayer under the influence of capillary waves and structural disorder (30). For the Gaussian model, Eq. 1 becomes

$$h_{\mathrm{pp}}(\kappa) = \frac{R\kappa^2}{16\pi^2 b_{\mathrm{L}}^2} = \Gamma^2\exp\left(-\frac{\kappa^2\sigma^2}{8}\right), \qquad (3)$$

where Γ is the surface excess and is equal to $1/(N_{\mathrm{a}}A)$ (N_{a} is the Avogadro constant). The width of Gaussian distribution

TABLE 2 Structural parameters obtained from fitting uniform layer models to neutron reflectivity profiles measured from d-DPPC monolayers spread on NRW

π/mN/m	A_{LT}/Å^2	A/Å^2	$\tau \pm 2$/Å	$\varpi \pm 1$/Å	$\sigma \pm 2$/Å	$\sigma' \pm 2$/Å
8	80 ± 10	70 ± 4	20	7.3	17.3	15.6
15	50 ± 6	55 ± 3	20	7.7	17.3	15.6
35	40 ± 4	45 ± 3	22	9.6	19.0	16.4

(σ) at the height of 1/e is 15% narrower than the thickness from the uniform layer. Fig. 4 compares the best fits using Eqs. 1 and 3. It can be seen that at the low and medium surface pressures of 8 and 15 mN/m, the Gaussian model fits the shape of the overall data better. However, at the high pressure of 35 mN/m the situation is opposite. A possible explanation is that over the low surface pressure region acyl chains are projected over a range of angles and there is a relatively large structural disorder within the layer. In comparison, the acyl chains are more ordered at the high surface pressure and the distribution of the segment density is better represented by the uniform layer slab.

In addition to the structural disorder the thickness measured from the lipid monolayer is also affected by the capillary waves arising from thermal agitation (30). The broadening contribution arising from the capillary waves (ϖ) can be estimated from the following equation

$$\sigma^2 = \sigma'^2 + \varpi^2, \tag{4}$$

where σ' is the intrinsic layer thickness after removal of capillary contribution. The structural parameters estimated for the Gaussian distribution before and after removal of capillary roughness are also given in Table 2. ϖ was estimated by assuming that its value was in inverse proportion to the square root of surface tension, taking into account the model-dependent factor of 2.3.

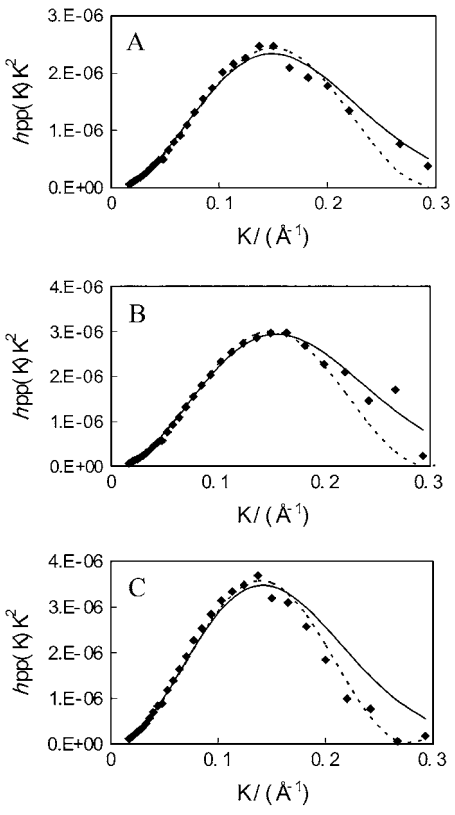

FIGURE 4 Comparison of the best uniform layer model (*dashed line*) and best Gaussian model (*continuous line*) fits to $h_{pp}(\kappa)\kappa^2$ measured from the d-DPPC monolayer on the surface of NRW at $\pi = 8$ (*A*), 15 (*B*), and 35 (*C*) mN/m.

It can be seen from Table 2 that despite the large variation of surface pressure and the accompanying change in *A*, the thickness varies very little, indicating little variation in the orientational order of the diacyl chains in the DPPC monolayer. Sun has elegantly modeled the structure of 1,2-dilignoceroylphosphatidylcholine (DLGPC) and has made careful comparisons with other phospholipids and with two saturated acyl chains, such as DPPC (31). Using molecular dynamics (MD) simulations Sun showed that the DLGPC/water monolayer in the condensed phase has the tilt angle of $\sim$30° with respect to surface normal and the hydrocarbon core thickness of the monolayer $\sim$28 Å. This would give the corresponding value of 17.5 Å for the dipalmitoyl chain region under the same angle of tilt and is consistent with the values close to 15.5–16.5 Å from our work, after removal of the capillary wave roughness contribution. Indeed, our thickness for the diacyl chain region also agrees well with the results from previous work by Helm et al. (32) and Naumann et al. (28). It is interesting to comment that the tilt angles of acyl chains in membrane lipid bilayers and multilayers have been found to vary between 15° and 25° by neutron reflection and x-ray studies (32–36), 15–30° by infrared (IR) studies (37,38), and 10–20° by sum-frequency vibrational spectroscopy (SFVS) (39). The range of these variations is large and appears to be instrument dependent due to their different sensitivities. There is likely to be differences in the acyl chain packing and orientation between lipid monolayer, bilayer, and multilayered structures, but it is difficult to find a clear trend from the existing data reported in the literature because of the limited number of systems studied and the possible complication relating to their different headgroups.

The zwitterionic DPPC headgroup is associated with water, and its distribution can be determined by measuring neutron reflectivity using h-DPPC in D_2O. As can be seen from Table 1 the scattering length density of the hydrogenated diacyl layer on top of the water surface is close to zero and is negligible. The measurement under this contrast thus provides a reliable determination of the thickness of the DPPC headgroup region. Fig. 5 shows the reflectivity profiles obtained at the three different surface pressures, and it can be seen that within experimental error the reflectivity profiles are broadly identical. The continuous line represents the best fit with a thickness of 9 Å and ρ of 3×10^{-6} Å^{-2}. The results thus indicate that within the surface pressure range studied the structure and composition of the headgroup region changes very little and that the headgroup remains within 9 $\pm$ 2 Å thick when these measured reflectivity profiles were best fitted individually. Taking into account the slightly narrower width among the Gaussian model and the contribution of capillary wave broadening, the actual headgroup thickness would be 7 $\pm$ 2 Å thick. There would also be some effects arising from surface packing density, but the

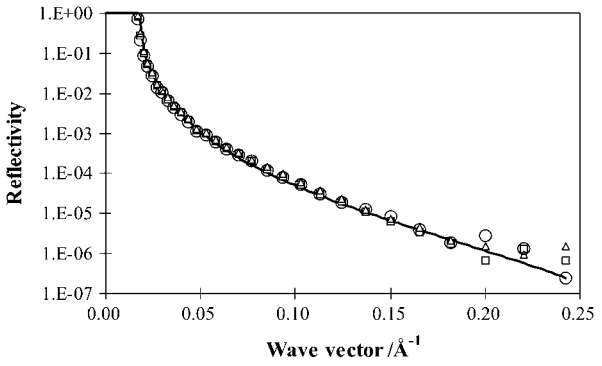

FIGURE 5 Neutron reflectivity profiles measured from surface adsorption of h-DPPC on D_2O surface at the surface pressure of 8 (*open circles*), 15 (*open triangles*), and 35 (*open squares*) mN/m. The continuous lines represent the best uniform layer fit with a thickness of 9 Å and scattering length density of 3×10^{-6} Å^{-2}.

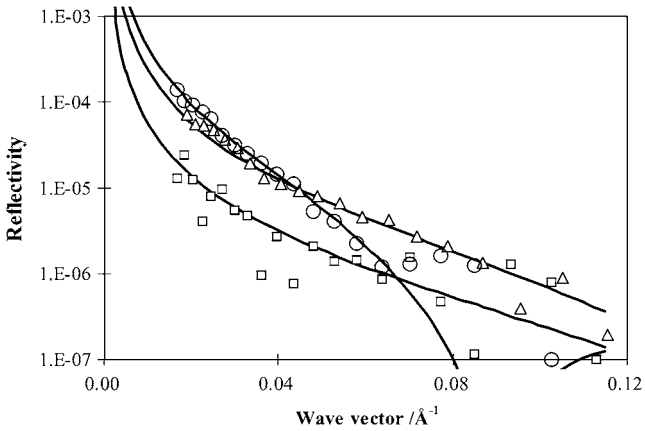

FIGURE 6 Neutron reflectivity profiles measured from surface adsorption of 0.1 mg/ml lactoferrin onto the h-DPPC monolayer spread on the NRW water surface at the surface pressure of 8 (*open circles*), 15 (*open triangles*), and 35 (*open squares*) mN/m. The continuous lines represent the best uniform layer fits with structural parameters listed in Table 3.

measurements with this isotopic combination clearly showed a lack of sensitivity to the concentration dependency. Nevertheless, the PC head layer thickness is consistent with the average values obtained from a number of previous studies for PC monolayers spread on the surface of water (28, 40). Pascher et al. estimated a value of 9 Å for the PC headgroup layer on the basis of the crystalline structure (41), indicating a tilt angle of 35° along the surface normal if the fully extended PC length was taken to be 11 Å. The thickness of our measured PC headgroup region is lower and the corresponding tile angle was ~50° and was rather consistent with the tilting as observed by Brumm et al. (40), also from neutron reflection. Measurements by other techniques such as NMR, IR, SFVS, and x-ray reflection also suggested the angle of tilting with respect to surface normal between 50° and 70° for the PC headgroup, indicating that the PC head would tend to stay flat on the surface (28,32–38,42). Note that despite self-consistency, neutron reflectivity is rather insensitive to the small changes in PC layer thickness, and a difference of ±1 Å could easily lead to an uncertainty of 10° in the tilt angle.

The coadsorption of lactoferrin into the spread DPPC monolayer was determined by neutron reflectivity using an isotopic combination of h-DPPC in NRW. As already shown in Table 1, the scattering length density of h-DPPC is so low that its contribution to reflectivity is negligible. Indeed, no measurable reflectivity was recorded when it was spread on NRW. Thus this isotopic combination provides a direct measure of the adsorption of the protein in the presence of the phospholipid monolayer. Fig. 6 shows the reflectivity profiles measured at three different initial surface pressures. They were measured within the first 2 h of injection of lactoferrin into the subphase. At the highest surface pressure of 35 mN/m there was little lactoferrin adsorption, consistent with the lack of change in the surface pressure. At the intermediate surface pressure of 15 mN/m some lactoferrin adsorption was detectable. At the lowest surface pressure of 8 mN/m more lactoferrin was found to adsorb. In addition, the layer thickness increased but the scattering length density decreased, indicating a protein volume fraction lower than that found at 15 mN/m. These observations thus indicated the variation of structural conformation with decreasing initial surface pressure; structural parameters of the adsorbed lactoferrin are reported in Table 3.

Furthermore, the time dependence of the lactoferrin adsorption was monitored, and Fig. 7 shows how the time dependence of the adsorption of lactoferrin affects the neutron reflectivity profiles measured at different time intervals. After the first 6 h the reflectivity was found not to vary with time, indicating that the coadsorption had reached equilibration.

Detailed data analysis showed that the first reflectivity profiles shown in Fig. 7 could be modeled by a uniform layer model. However, the reflectivity profiles measured after 6 h and onward had to be approximated by a two-layer model to accommodate the structural inhomogeneity along the surface normal direction. The structural parameters obtained from the model analysis are listed in Table 4.

It should be noted that during the first 3 h of the experiment the surface pressure was increased from the initial 8 mN/m to 15 mN/m and by the fifth to sixth hour the surface pressure tended to a plateau of 18 mN/m. Table 4 clearly shows a steady increase of protein adsorption with surface

TABLE 3 The structural parameters obtained from coadsorption of lactoferrin onto spread h-DPPC monolayer at different surface pressures

π/mN/m	$(\rho \pm 0.05)/10^{-6}$ Å^{-2}	τ/Å	A/Å^2
8	0.24	70 ± 8	11,300 ± 1200
15	0.35	35 ± 3	15,500 ± 1600
35	0.15	30 ± 3	42,200 ± 6000

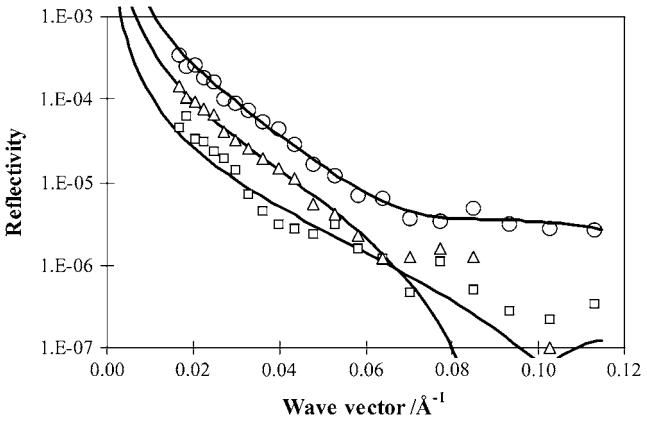

FIGURE 7 Neutron reflectivity profiles measured from surface adsorption of 0.1 mg/ml lactoferrin onto the h-DPPC monolayer spread on the NRW water surface at the surface pressure of 8 mN/m. The reflectivity profiles were measured within the first hour (*open squares*), third hour (*open triangles*), and sixth hour (*open circles*) after the injection of 0.1 mg/ml lactoferrin in the subphase. The continuous lines represent the best uniform layer fits with structural parameters listed in Table 4.

pressure. An important observation from Table 4 is the change of protein layer structure during the course of time-dependent adsorption. Within the first 2–3 h the layer became thickened and its volume fraction also increased. However, from 4 h onward it became necessary to model the reflectivity by a two-layer model rather than the single uniform layer model to accommodate the increased nonuniform density distribution of lactoferrin within the adsorbed layer. The reflectivity profile measured during 5–6 h intervals was represented by a top sublayer of 15 Å with a protein volume fraction of 0.54 and a bottom diffuse sublayer of 60 Å with a protein volume fraction of 0.1. The structural distribution is characteristic of the feature of lactoferrin adsorption at the air/water interface free of the phospholipid monolayer (26).

Lactoferrin is a bilobal globular protein. Each lobe has the dimensions of $55 \times 35 \times 35$ Å^3. The two lobes are jointed by an α-helical connection. Because the top dense layer is significantly thinner than the short axial length of 35 Å, the results indicated structural unfolding of their globular framework. Although the main feature of the unfolded structural distribution is the same as in the absence of the phospholipid monolayer, the top dense sublayer in the presence of the phospholipid monolayer is rather thinner. The thickness and the volume fraction of the diffuse sublayers are nevertheless similar. The overall effect is that the net amount of protein adsorption is reduced by the presence of a phospholipid monolayer.

TABLE 4 The structural parameters obtained from the time-dependent coadsorption of 0.1 mg/ml lactoferrin onto the spread h-DPPC monolayer at the surface pressure of 8 mN/m

Time/h	π/mN/m	$(\rho \pm 0.05)/10^{-6}$ Å^{-2}	τ/Å	A/Å^2
0–1	8–12	0.17	50 ± 6	22,300 ± 2500
1–2	12–15	0.24	70 ± 8	11,300 ± 1200
5–6	19–20	(a) 1.1	15 ± 2	11,500 ± 1200
		(b) 0.2	60 ± 7	15,800 ± 1500

The almost identical structural distribution of lactoferrin on the surface suggests that in the current situation lactoferrin must have penetrated into the DPPC monolayer and is also likely to have direct exposure to the outer air surface. Previous study has revealed that the top dense sublayer is predominantly projected in air at a simple air/water interface (26). In the presence of the hydrophobic diacyl chain region on the outer surface, it is reasonable to assume that the top dense sublayer is intermixed with the hydrocarbon chains. This result is consistent with the observation of in-plane interactions between protein and the phospholipid monolayer under the same surface pressure of 8 mN/m as revealed by BAM and GIXD (21,29). It should, however, be noted that at this surface pressure structural unfolding did not occur until several hours after lactoferrin injection. This clearly suggests that the structural unfolding at the interface was time dependent, an observation also consistent with the results reported by Zhao et al. in their BAM study (29).

CONCLUSIONS

Although the kinetic and equilibrium properties of the coadsorption of protein into phospholipid monolayer have been extensively studied by techniques such as BAM, fluorescence microscopy, and GIXD, little information is available about the relative amount and structural distribution of the protein layers accompanying the time-dependent changes in surface pressure. Neutron reflectivity measurements complement these existing studies by determining the structural distributions of protein under an increasingly tight-packed phospholipid monolayer. The selection of a range of isotopic combinations was found to be extremely advantageous for revealing structural information of the protein without any practical interference arising from the phospholipid monolayer.

The thickness determined from d-DPPC in NRW showed that whereas the area per molecule varied from 40 Å^2 to 70 Å^2 in response to the variation in surface pressure, the thickness of the acyl chain region varied little. The almost constant thickness of 16 Å is consistent with the previous experimental reports by others and is also consistent with the proportion of the projection of much longer acyl chains in the same homolog as predicted by MD simulation (31), indicating an almost constant tilting of 30° for the acyl chains away from the surface normal. The thickness of the PC headgroup region was determined from h-DPPC in D_2O, as the almost zero scattering length density of the hydrogenated acyl chains on the air surface makes little contribution. The PC headgroup region was found to be 9 ± 2 Å thick for a uniform layer model and was estimated to be 7 ± 2 Å thick for a Gaussian model. The reflectivity profiles showed little change with

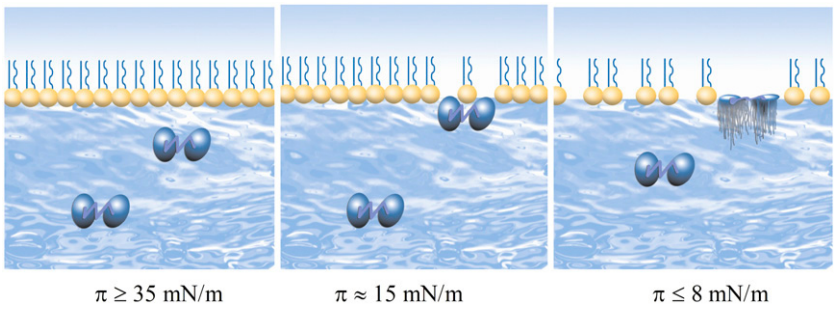

FIGURE 8 Schematic representation of lactoferrin coadsorption into the DPPC monolayer with increasing surface pressure.

changes in surface pressure or the area per molecule, showing an invariance of the packing of the PC headgroups similar to the case of the diacyl chains.

Fig. 8 shows a schematic representation of lactoferrin coadsorption into the DPPC monolayer with increasing surface pressure. The amount of lactoferrin adsorbed and its penetration into the phospholipid monolayer was found to increase with decreasing applied surface pressure. Furthermore, as the initial surface pressure decreased the structural distribution of the adsorbed protein layer also changed. More protein adsorption was associated with longer time-dependent interfacial behavior, indicating further structural reorientation. The observation of rising surface pressure was accompanied by the increasing lactoferrin adsorption as confirmed by the neutron reflectivity measurements. After this initial period the adsorbed protein layer was characterized by two distinct regions: a top dense sublayer of 15 Å containing nearly 50% protein and a bottom sublayer of 70 Å containing 10% protein phase. This structural profile is the same as that revealed at the air/water interface without a phospholipid monolayer, clearly indicating the unfolding of the globular framework.

The system studied in this work was assumed as a model for the tear film outer interface characterized by the presence of a thin (200 nm) insoluble lipid layer spread upon a protein-rich aqueous subphase where lactoferrin is particularly abundant (3). The observations made in this in vitro model concern the ability of a densely packed lipid interface to prevent protein's coadsorption where the possible insertion of proteins at the interface will determine a progressive loss of tertiary structure and consequent degradation of the protein itself. Conversely, a nonuniform or weakly packed lipid layer was found to allow protein coadsorption and the setup of a lipid/protein mixed interface. The above considerations will be taken into account when mimicking the biological system where the lipid layer, standing at the top of the tear film, contains amphiphilic components such as phospholipids, ceramides, and cerebrosides and nonpolar molecules such as cholesterol esters, fatty acid esters, and triglycerides, all of them contributing to the interfacial properties of the film (43).

A further step to model the biological system is the diffractive investigation of the structure of natural meibomian lipids at the air/aqueous interface. Some authors have already presented preliminary results of grazing incidence x-ray diffraction (GIXD) from the surface lipid layer of the preocular tear film in which a 2D order was found to contain typical spacings of 3.75 Å and 4.16 Å, independent of the monolayer surface pressure (F. Miano, P. G. Petrov, and C. P. Winlove, unpublished data, presented at the Condensed Matter and Material Physics Conference, 2006). Further neutron reflection work will focus on the investigation of the modifications of the meibomian lipid structure at the air/aqueous interface in the presence of tear proteins. We believe that the establishment of a protein-meibomian lipid mixed layer model, where protein coadsorption is manifested, will allow the modifications of the native structure of coadsorbed proteins and the consequent physiology of the tear film, thus contributing to the emergence of dry eye conditions to be studied. In view of these results, a new therapeutic approach of supplementing lipids in the form of emulsions, already seen as an effective restructuring of the preexisting lipid film (44), gains a further physically based rationale.

We acknowledge the funding support from Società Industria Farmaceutica Italiana SpA, Biotechnology and Biological Sciences Research Council, UK, and Engineering and Physical Sciences Research Council, UK.

REFERENCES

1. Wolff, E. 1946. The mucocutaneous junction of the lid margin and the distribution of the tear fluid. *Trans Ophthalm. Soc UK*. 66:291–308.
2. Korb, D. R., J. Craig, M. Doughty, J. P. Guillon, G. Smith, and A. Tomlinson. 2002. The Tear Film: Structure, Function and Clinical Examination. Butterworth & Heinemann, London.
3. Fullard, R. J., and C. Snyder. 1990. Protein levels in nonstimulated and stimulated tears of normal human subjects. *Invest Ophth. Vis. Sci.* 31: 1119–1126.
4. Gachon, A. F., and E. Lacazette. 1998. Tear lipocalin and the eye's front line of defence. *Br. J. Ophthalmol.* 82:453–455.
5. Tiffany, J. M. 1987. The lipid secretion of the meibomian glands. *Adv. Lipid Res.* 22:1–62.
6. Craig, J. P., and A. Tomlinson. 1997. Importance of the lipid layer in the human tear film stability and evaporation. *Optom. Vis. Sci.* 74: 8–13.
7. Goto, E., K. Endo, A. Suzuki, Y. Fujikura, Y. Matsumoto, and K. Tsubota. 2003. Tear evaporation dynamics in normal subjects and subjects with obstructive meibomian gland dysfunction. *IOVS*. 44:2, 533–539.

8. Miano, F., M. Calcara, F. Giuliano, T. J. Millar, and V. Enea. 2004. Effect of meibomian lipid layer on evaporation of tears. *J. Phys. Condens. Matter*. 16:S2461–S2467.
9. Kaercher, T., D. Mobius, and R. Welt. 1994. Biophysical behaviour of the infant meibomian lipid layer. *Int. Ophthalmol.* 18:15–19.
10. McCulley, J. P., and W. E. Shine. 2001. The lipid layer: the outer surface of the ocular surface tear film. *Biosci. Rep.* 21:407–418.
11. Miano, F., M. Calcara, T. J. Millar, and V. Enea. 2005. Insertion of tear proteins into a meibomian lipids film. *Colloid Surf. B.* 44:49–55.
12. Glasgow, B. J., G. Marshall, O. K. Gasymov, A. R. Abduragimov, T. N. Yusifov, and C. M. Knobler. 1999. Tear lipocalins: potential lipid scavenger for the corneal surface. *Invest. Ophthalmol. Vis. Sci.* 40: 3100–3107.
13. Perez-Gil, J., K. Nag, S. Taneva, and K. M. Keough. 1992. Pulmonary surfactant protein SP-C causes packing rearrangements of dipalmitoylphosphatidylcholine in spread monolayers. *Biophys. J.* 63:197–204.
14. Ruano, M. L. F., K. Nag, L. A. Worthman, C. Casals, J. Pérez-Gil, and K. M. W. Keough. 1998. Differential partitioning of pulmonary surfactant protein SP-A into regions of monolayers of dipalmitoylphosphatidylcholine and dipalmitoylphosphatidylcholine/dipalmitoylphosphatidyl glycerol. *Biophys. J.* 74:1101–1109.
15. Worthman, L. D., N. Kaushok, N. Rich, M. L. F. Ruano, C. Casals, J. Perez-Gil, and K. M. W. Keough. 2000. Pulmonary surfactant protein *A* interacts with gel-like regions in monolayers of pulmonary surfactant lipid extract. *Biophys. J.* 79:2657–2686.
16. Holly, F. J. 1974. Surface chemistry of tear component analogs. *J. Coll. Interface Sci.* 49:221–231.
17. Miano, F., M. G. Mazzone, A. Giannetto, V. Enea, A. Bailey, P. McCulley, and P. Winlove. 2002. Interface properties of simplified tear-like fluids in relation to lipid and aqueous layer composition. *Adv. Exp. Med. Biol.* 506:405–417.
18. Borchman, D., L. Huang, D. Tang, G. R. John, and M. C. Yappert. 2002. The composition, structure and protein interactions of human tear film lipid. 2002 Investigative Ophthalmology & Visual Science Meeting Abstracts. Investigative Ophthalmology & Visual Science. Supplement, 43, Abstract, 81.
19. Dinslage, S., W. Stoffel, M. Diestelhorst, and G. K. Krieglstein. 2002. Tolerability and safety of two new preservative-free tear film substitutes. *Cornea*. 21:352–355.
20. Sugar, I. P., N. K. Mizuno, and H. L. Brockman. 2005. Peripheral protein adsorption to lipid-water interfaces: the free area theory, *Biophys. J.* 89:3997–4005.
21. Vollhardt, D., and V. B. Fainerman. 2000. Penetration of dissolved amphiphiles into two-dimensional aggregating lipid monolayers. *Adv. Colloid Interface Sci.* 86:106–151.
22. Zhang, H., G. Cui, and J. Li. 2002. Morphological investigation of mixed protein/phospholipids monolayers. *Coll. Surf. A: Physicochem. Eng. Asp.* 201:123–129.
23. Bellamy, W., M. Takase, K. Yamauchi, H. Wakabayashi, K. Kawase, and M. Tomita. 1992. Identification of the bactericidal domain of lactoferrin. *Biochim. Biophys. Acta*. 1121:130–136.
24. Ohashi, Y., R. Ishida, T. Kojima, E. Goto, Y. Matsumoto, K. Watanabe, N. Ishida, K. Nakata, T. Takeuchi, and K. Tsubota. 2003. Abnormal protein profiles in tears with dry eye syndrome. *Am. J. Ophthalmol.* 136:291–299.
25. Dalmasso, E. A., A. Wirthlin, and N. Pfeiffer. 2005. SELDI-TOF-MS protein chip array profiling of tears from patients with dry eye. *IOVS*. 46:863–876.
26. Lu, J. R., S. Perumal, X. Zhao, F. Miano, V. Enea, R. R. Heenan, and J. Penfold. 2005. Surface-induced unfolding of human lactoferrin. *Langmuir*. 21:3354–3361.
27. Lu, J. R., T. J. Su, P. N. Thirtle, R. K. Thomas, A. R. Rennie, and R. Cubitt. 1998. The denaturation of lysozyme layers adsorbed at the hydrophobic solid/liquid interface studied by neutron reflection. *J. Colloid Interface Sci.* 206:212–223.
28. Naumann, C., C. Dietrich, J. R. Lu, R. K. Thomas, A. R. Rennie, J. Penfold, and T. M. Bayerl. 1994. Structure of mixed monolayers of dipalmitoylglycerophosphocholine and polyethylene glycol monododecyl ether at the air/water interface determined by neutron reflection and film balance techniques. *Langmuir*. 10:1919–1925.
29. Zhao, J., D. Vollhardt, G. Brezesinski, S. Siegel, J. Wu, J. B. Li, and R. Miller. 2000. Effect of protein penetration into phospholipid monolayers: morphology and structure. *Colloid Surf. A Physicochem. Eng. Asp.* 171:175–184.
30. Lu, J. R., R. K. Thomas, and J. Penfold. 2000. Surfactant layers at the air/water interface: structure and composition. *Adv. Colloid Interface Sci.* 84:143–304.
31. Sun, F. 2002. Constant normal pressure, constant surface tension, and constant temperature molecular dynamics simulation of hydrated 1,2-dilignoceroylphosphatidylcholine monolayer. *Biophys. J.* 82:2511–2519.
32. Helm, C. A., H. Mohwald, K. Kjaer, and J. Als-Nielsen. 1987. Phospholipid monolayer density distribution perpendicular to the water surface. A synchrotron x-ray reflectivity study. *Europhys. Lett.* 4:697–703.
33. Janiak, M. J., D. M. Small, and G. G. Shipley. 1976. Nature of thermal pretransition of synthetic phospholipids: dimyristoyl- and dipalmitoyllecithin. *Biochemistry.* 15:4575–4580.
34. Tardieu, A., V. Luzzati, and F. C. Reman. 1973. Structure and polymorphism of the hydrocarbon chains of lipids: a study of lecithin-water phases. *J. Mol. Biol.* 75:711–718.
35. McIntosh, T. J., and S. A. Simon. 1993. Contributions of hydration and steric (entropic) pressures to the interactions between phosphatidylcholine bilayers: experiments with the subgel phase. *Biochemistry.* 32: 8374–8384.
36. Pearson, R. H., and I. Pascher. 1979. The molecular structure of lecithin dihydrate. *Nature*. 281:499–501.
37. Binder, H., T. Gutberlet, A. Anikin, and G. Klose. 1998. Hydration of the dienic lipid octadecadienoylphosphatidylcholine in the lamellar phase: an infrared linear dichroism and x-ray study on headgroup orientation, water ordering, and bilayer dimensions. *Biophys. J.* 74: 1908–1923.
38. Hubner, W., and H. H. Mantsch. 1991. Orientation of specifically $^{13}C{=}O$ labelled phosphatidylcholine multilayers from polarized attenuated total reflection FT-IR spectroscopy. *Biophys. J.* 59:1261–1272.
39. Liu, J., and J. C. Conboy. 2005. Structure of a gel phase lipid bilayer prepared by the Langmuir-Blodgett/Langmuir-Schaefer method characterised by sum-frequency vibrational spectroscopy. *Langmuir.* 21: 9091–9097.
40. Brumm, T., C. Naumann, E. Sackmann, A. R. Rennie, R. K. Thomas, D. Kanellas, J. Penfold, and T. M. Bayerl. 1994. Conformational changes of the lecithin headgroup in monolayers at the air/water interface. *Eur. Biophys. J.* 23:289–295.
41. Pascher, I., S. Sundell, K. Harlos, and H. Eibl. 1987. Conformation of packing properties of lipids: the crystal structure of sodium DMPG. *Biochim. Biophys. Acta*. 896:77–88.
42. Büldt, G., H. U. Gally, J. Seelig, and G. Zaccai. 1979. Neutron diffraction studies on phosphatidylcholine model membranes: I. Head group conformation. *J. Mol. Biol.* 134:673–691.
43. Nagyova, B., and J. M. Tiffany. 1999. Components responsible for the surface tension of human tears. *Curr. Eye Res.* 19:4–11.
44. Di Pascuale, M. A., E. Goto, and S. C. Tseng. 2004. Sequential changes of lipid tear film after the instillation of a single drop of a new emulsion eye drop in dry eye patients. *Ophthalmology.* 111:783–791.